Int. J. Solids Structures, 1974, 10, pp. 61–76. Pergamon Press. Printed in Gt. Britain.

WAVE PROPAGATION IN ELASTIC LAMINATES USING A SECOND ORDER MICROSTRUCTURE THEORY†

D. S. DRUMHELLER

Sandia Laboratories, Albuquerque, New Mexico 87115

and

A. BEDFORD

Department of Aerospace Engineering and Engineering Mechanics University of Texas, Austin, Texas 78712

(*Received* 3 *March* 1973)

Abstract—A generalization of the simpler microstructure theory developed earlier for elastic laminates by Sun, Achenbach and Herrmann is used to analyze steady state plane wave propagation. This new version incorporates higher-order thickness variations in the displacement functions and includes restrictions on both displacement and stress at the laminate interfaces.

To assess the potential of a second-order microstructure theory for accurate modeling of mechanical processes in laminates, dispersion results and especially mode shape data for both displacements and stresses are obtained and compared to corresponding solutions obtained by the theory of elasticity. The comparisons indicate that while dispersion results may be nearly identical, extremely significant differences may be observed in the mode shapes.

1. INTRODUCTION

The development of a practical technique for the numerical solution of problems in the mechanics of composite materials is a problem of great importance to designers using such materials. One approach to this problem is by numerical solution of the equations arising from a continuum microstructure theory of composite materials. The objective of this paper is to provide a preliminary indication of the feasibility of such an approach.

Two microstructure theories of composite materials have been developed to the point that they would be suitable for this study. The first such theory, the effective stiffness theory of Sun, Achenbach and Herrmann[1–7], is based on expressing the displacement vector in each layer as a series expansion about the centerline of that layer. The coefficients of the expansions constitute the microstructure variables of the theory. An interface compatibility equation is introduced which ensures that the displacements of adjacent layers agree at the interfaces. Then, by writing the strain and kinetic energies of the layers in terms of the displacement expansions, "smoothing" the resulting expressions to obtain continuous variables, and applying Hamilton's principle, a continuum theory is obtained.

A second microstructure theory for composites has been developed by Hegemier *et al.*[8]. This theory also uses displacement vector expansions. However, the equations of motion and constitutive equations are then used together with the interface stress and displacement compatibility equations to obtain finite-difference equations which are used to derive the

† This work was supported by the United States Atomic Energy Commission.

differential equations of the theory. Its only essential difference from the effective stiffness theory is that, rather than leading to microstructure variables, it results in equations containing higher-order gradients in the displacements, in the manner of a material of grade N[9].

For the purpose of this study, we have used a version of the effective stiffness theory[10] which generalizes the original theory in two ways: (1) A procedure was introduced which permits the systematic derivation of the compatibility equations at layer interfaces for the generation of theories of arbitrary order.† (2) Interface compatibility requirements were introduced for matching stresses as well as displacements. Thus, a theory was obtained which can systematically be extended to arbitrary order and which can model stresses in the composite constituents.

The theory is used to investigate the propagation of steady state waves at an arbitrary angle to the laminate interfaces. This type of calculation has been carried out previously for dispersion characteristics, for example by Sve who obtained dispersion spectra for the first-order effective stiffness theory[11]. However, the emphasis in our study is not merely on dispersion characteristics but also on the capability of a continuum system of higher order microstructure equations to model mode shapes of both displacements and stresses. To demonstrate this, we have made comparisons with corresponding solutions from a discrete system of elasticity equations. It is this mode description, rather than only dispersion data, which is essential to illustrate the potential of the theory to model stresses and displacements arising in mechanical processes in composites. This ability of the theory must be assessed prior to attempting numerical solutions of specific problems, and provides the motivation for this paper.

The foundations of the effective stiffness theory and the second-order generalization developed in [10] will first be briefly reviewed, and the general equations for plane–strain motion derived. Wave propagation results are then presented and interpreted in comparison with corresponding exact elasticity solutions.

2. EQUATIONS OF MOTION

The material considered is a laminate of perfectly bonded alternating plane layers of two elastic materials (Fig. 1). One material, the matrix, has density ρ_m and Lamé constants λ_m, μ_m and the other material, the reinforcing, has density ρ_f, μ_f.‡

A Cartesian coordinate system is oriented so that the x_2 axis is normal to the layers and the x_1, x_3 axes are in the plane of the layers. Only plane-strain motion in the x_1–x_2 plane is considered.

The expansion for the displacement vector in the kth reinforcing layer, ${u_i}^{fk}$, $i = 1, 2$, is, for a second-order theory[1]

$$ {u_i}^{fk} = {u_{0i}}^{fk}(x_1, {x_2}^{fk}, t) + \bar{x}_2{}^f {\psi_i}^{fk}(x_1, {x_2}^{fk}, t) + \tfrac{1}{2}(3\bar{x}_2{}^{f2} - {d_f}^2){\phi_i}^{fk}(x_1, {x_2}^{fk}, t) \quad (1) $$

where ${\psi_i}^{fk}$ and ${\phi_i}^{fk}$ are first- and second-order microdisplacements, ${x_2}^{fk}$ is the x_2 coordinate of the kth reinforcing layer centerline, $\bar{x}_2{}^f$ is the distance in the $\bar{x}_2$ direction from the layer centerline, and d_f is the layer thickness.

By substituting equation (1) into the usual isotropic linearly elastic constitutive equation,

† By the "order" of an effective stiffness theory we denote the number of terms retained in the displacement vector expansions; one term is a zero-order theory, two terms a first-order theory, etc.

‡ The notation is consistent with [1–7].

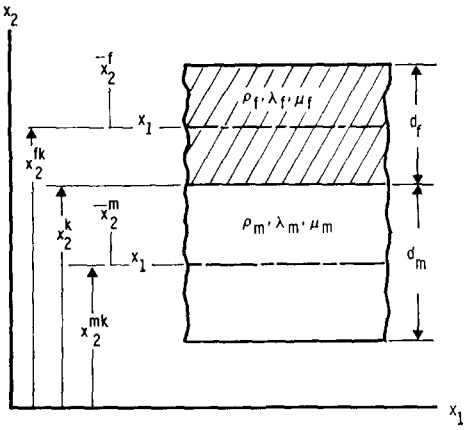

Fig. 1. Laminated medium.

the stress components in the kth reinforcing layer can be written in terms of microdisplacements. In [10], equation (1) and the stress component expressions were used to derive interface compatibility equations expressing the equality of displacement and stress at interfaces between adjacent layers. The resulting displacement compatibility equations are

$$u_{0i}{}^f + \tfrac{1}{8}d_f{}^2 u^f_{0i,22} - \tfrac{1}{4}d_f{}^2\psi^f_{i,2} - \tfrac{1}{8}d_f{}^2\Phi_i{}^f = u_{0i}{}^m + \tfrac{1}{8}d_m{}^2 u^m_{i,22} - \tfrac{1}{4}d_m{}^2\psi^m_{i,2} - \tfrac{1}{8}d_m{}^2\Phi_i{}^m \quad (2)$$

$$-\tfrac{1}{2}d_f u^f_{0i,2} + \tfrac{1}{2}d_f\psi_i{}^f = \tfrac{1}{2}d_m u^m_{0i,2} - \tfrac{1}{2}d_m\psi_i{}^m \quad (3)$$

where j (subscript) denotes partial differentiation with respect to x_j, and the stress compatibility equations are

$$\begin{aligned} E_f(\psi_2{}^f + \tfrac{1}{8}d_f{}^2\psi^f_{2,22} - \tfrac{3}{4}d_f{}^2\Phi_{2,2}) + \lambda_f(u^f_{01,1} + \tfrac{1}{8}d_f{}^2 u^f_{01,122} - \tfrac{1}{4}d_f{}^2\psi^f_{1,12} \\ - \tfrac{1}{8}d_f{}^2\Phi^f_{1,1}) = E_m(\psi_2{}^m + \tfrac{1}{8}d_m{}^2\psi^m_{2,22} - \tfrac{3}{4}d_m{}^2\Phi^m_{2,2}) \\ + \lambda_m(u^m_{01,1} + \tfrac{1}{8}d_m{}^2 u^m_{01,122} - \tfrac{1}{4}d_m{}^2\psi^m_{1,12} - \tfrac{1}{8}d_m{}^2\Phi^m_{1,1}). \end{aligned} \quad (4)$$

$$\begin{aligned} E_f(-\tfrac{1}{2}d_f\psi^f_{2,2} + \tfrac{3}{2}d_f\Phi_2{}^f) + \lambda_f(-\tfrac{1}{2}d_f u^f_{01,12} + \tfrac{1}{2}d_f\psi^f_{1,1}) \\ = E_m(\tfrac{1}{2}d_m\psi^m_{2,2} - \tfrac{3}{2}d_m\Phi_2{}^m) + \lambda_m(\tfrac{1}{2}d_m u^m_{01,12} - \tfrac{1}{2}d_m\psi^m_{1,1}). \end{aligned} \quad (5)$$

$$\begin{aligned} \mu_f(\psi_1{}^f + \tfrac{1}{8}d_f{}^2\psi^f_{1,22} - \tfrac{3}{4}d_f{}^2\Phi^f_{1,2} + u^f_{02,1} + \tfrac{1}{8}d_f{}^2 u^f_{02,122} - \tfrac{1}{4}d_f{}^2\psi^f_{1,12} \\ - \tfrac{1}{8}d_f{}^2\Phi^f_{2,1}) = \mu_m(\psi_1{}^m + \tfrac{1}{8}d_m{}^2\psi^m_{1,22} - \tfrac{3}{4}d_m{}^2\Phi^m_{1,2} + u^m_{02,1} + \tfrac{1}{8}d_m{}^2 u^m_{02,122} \\ - \tfrac{1}{4}d_m{}^2\psi^m_{2,12} - \tfrac{1}{8}d_m{}^2\Phi^m_{2,1}). \end{aligned} \quad (6)$$

$$\begin{aligned} \mu_f(-\tfrac{1}{2}d_f\psi^f_{1,2} + \tfrac{3}{2}d_f\Phi_i{}^f - \tfrac{1}{2}d_f u^f_{02,12} + \tfrac{1}{2}d_f\psi^f_{2,1}) \\ = \mu_m(\tfrac{1}{2}d_m\psi^m_{1,2} - \tfrac{3}{2}d_m\Phi_1{}^m + \tfrac{1}{2}d_m u^m_{02,12} - \tfrac{1}{2}d_m\Phi^m_{2,1}), \end{aligned} \quad (7)$$

where $u_{0i}{}^f$, $u_{0i}{}^m$, $\psi_i{}^f$, $\psi_i{}^m$, $\phi_i{}^f$ and $\phi_i{}^m$ are continuous variables corresponding to the discrete variables $u_{0i}{}^{fk}$, $u_{0i}{}^{mk}$, $\psi_i{}^{fk}$, $\psi_i{}^{mk}$, $\phi_i{}^{fk}$ and $\phi_i{}^{mk}$, and where $E_f = \lambda_f + 2\mu_f$, $E_m = \lambda_m + 2\mu_m$.

Note that, when second-order terms in d_f, d_m are neglected, equations (2) and (3) reduce to the displacement compatibility equations used by Sun, Achenbach and Herrmann[1–7].

The equations of motion for the theory are obtained using the procedure introduced in [1]. By substituting equation (1) into the usual expression for the elastic strain energy in

terms of displacements and integrating the resulting expression with respect to $\bar{x}_2{}^f$ from $-d_f/2$ to $d_f/2$, the strain energy per unit area of the kth reinforcing layer, $W_A{}^{fk}$, is

$$\begin{aligned} W_A{}^{fk} = {} & \tfrac{1}{2}E_f(d_f u_{01,1}^{fk2} + \tfrac{1}{12}d_f{}^3\psi_{1,1}^{fk2} + \tfrac{49}{320}d_f{}^5\Phi_{1,1}^{fk2} \\ & - \tfrac{3}{4}d_f{}^3u_{01,1}^{fk}\Phi_{1,1}^{fk} + d_f\psi_2{}^{fk2} + \tfrac{3}{4}d_f{}^3\Phi_2{}^{fk2}) \\ & + \lambda_f(d_f u_{01,1}^{fk}\psi_2{}^{fk} + \tfrac{1}{4}d_f{}^3\psi_{1,1}^{fk}\Phi_2{}^{fk} - \tfrac{3}{8}d_f{}^3\Phi_{1,1}^{fk}\psi_2{}^{fk}) \\ & + \frac{\mu_f}{2}(d_f\psi_1{}^{fk2} + \tfrac{3}{4}d_f{}^3\Phi_1{}^{fk2} + d_f u_{02,1}^{fk2} + \tfrac{1}{12}d_f{}^3\psi_{2,1}^{fk2} \\ & + \tfrac{49}{320}d_f{}^5\Phi_{2,1}^{fk2} + 2d_f\psi_1{}^{fk}u_{02,1}^{fk} - \tfrac{3}{4}d_f{}^3\psi_1{}^{fk}\Phi_{2,1}^{fk} \\ & + \tfrac{1}{2}d_f{}^3\Phi_1{}^{fk}\psi_{2,1}^{fk} - \tfrac{3}{4}d_f{}^3u_{02,1}^{fk}\Phi_{2,1}^{fk}), \end{aligned} \tag{8}$$

with a corresponding expression $W_A{}^{mk}$ for the kth matrix layer.

Similarly, the kinetic energy per unit area of the kth reinforcing layer, $T_A{}^{fk}$, is

$$\begin{aligned} T_A{}^{fk} = {} & \tfrac{1}{2}\rho_f(d_f\dot{u}_{01}{}^{fk2} + \tfrac{1}{12}d_f{}^3\dot{\psi}_1{}^{fk2} + \tfrac{49}{320}d_f{}^5\dot{\Phi}_1{}^{fk2} \\ & - \tfrac{3}{4}d_f{}^3\dot{u}_{01}{}^{fk}\Phi_1{}^{fk} + d_f\dot{u}_{02}{}^{fk2} + \tfrac{1}{12}d_f{}^3\dot{\psi}_2{}^{fk2} \\ & + \tfrac{49}{320}d_f{}^5\dot{\Phi}_2{}^{fk2} - \tfrac{3}{4}d_f{}^3\dot{u}_{02}{}^{fk}\Phi_2{}^{fk}), \end{aligned} \tag{9}$$

where $(\dot{})$ denotes differentiation with respect to time with a corresponding expression $T_A{}^{mk}$ for the kth matrix layer.

To obtain the continuum theory, the discrete energies $W_A{}^{fk}$, $W_A{}^{mk}$, $T_A{}^{fk}$, $T_A{}^{mk}$ are replaced by the continuous functions

$$W = (W_A{}^f + W_A{}^m)/h, \tag{10}$$

$$T = (T_A{}^f + T_A{}^m)/h, \tag{11}$$

where $W_A{}^m$, $W_A{}^f$, $T_A{}^m$, $T_A{}^f$ denote the discrete functions $W_A{}^{mk}$, $W_A{}^{fk}$, $T_A{}^{mk}$, $T_A{}^{fk}$ with the discrete functions $u_{01}{}^{fk}$, $u_{01}{}^{mk}$, ... replaced by the corresponding continuous functions $u_{01}{}^f$, $u_{01}{}^m$, ..., and where $h = d_f + d_m$.

With the continuous energy functions (10) and (11), a Lagrangian can be defined from which displacement equations of motion can be obtained through Hamilton's principle. As in [1] the interface compatibility equations are included in the Lagrangian through the introduction of Lagrange multipliers. Denoting the eight compatibility equations (2)–(7) by $F_j = 0, j = 1, 2, \ldots, 8$, the Lagrangian is

$$L = T - W - \sum_{j=1}^{8}\lambda_j F_j, \tag{12}$$

where the λ_j are Lagrange multipliers. Using the appropriate Euler equation for a Lagrangian involving third derivatives in the dependent variables, equation (12) leads to the equations

$$\begin{aligned} & \lambda_1 - \frac{\rho_m d_m}{h}\ddot{u}_{01}{}^m + \frac{3}{8}\frac{\rho_m d_m{}^3}{h}\ddot{\phi}_1{}^m + \frac{E_m d_m}{h}u_{01,11}^m - \frac{3}{8}\frac{E_m d_m{}^3}{h}\phi_{1,11}^m + \frac{\lambda_m d_m}{h}\psi_{2,1}^m \\ & - \lambda_m\lambda_{5,1} - \tfrac{1}{2}d_m\lambda_{3,2} + \tfrac{1}{2}\lambda_m d_m\lambda_{6,12} + \tfrac{1}{8}d_m{}^2\lambda_{1,22} \\ & - \tfrac{1}{8}\lambda_m d_m{}^2\lambda_{5,122} = 0. \end{aligned} \tag{13}$$

$$\begin{aligned} & -\lambda_1 - \frac{\rho_f d_f}{h}\ddot{u}_{01}{}^f + \frac{3}{8}\frac{\rho_f d_f{}^3}{h}\ddot{\phi}_1{}^f + \frac{E_f d_f}{h}u_{01,11}^f - \frac{3}{8}\frac{E_f d_f{}^3}{h}\phi_{1,11}^f + \frac{\lambda_f d_f}{h}\psi_{2,1}^f \\ & + \lambda_f\lambda_{5,1} - \tfrac{1}{2}d_f\lambda_{3,2} + \tfrac{1}{2}\lambda_f d_f\lambda_{6,12} - \tfrac{1}{8}d_f{}^2\lambda_{1,22} + \tfrac{1}{8}\lambda_f d_f{}^2\lambda_{5,122} = 0. \end{aligned} \tag{14}$$

$$\lambda_2 - \frac{\rho_m d_m}{h}\ddot{u}_{02}{}^m + \frac{3}{8}\frac{\rho_m d_m{}^3}{h}\ddot{\phi}_2{}^m + \frac{\mu_m d_m}{h}u^m_{02,11} - \frac{3}{8}\frac{\mu_m d_m{}^3}{h}\phi^m_{2,11} + \frac{\mu_m d_m}{h}\psi^m_{1,1}$$
$$- \mu_m\lambda_{7,1} - \tfrac{1}{2}d_m\lambda_{4,2} + \tfrac{1}{2}\mu_m d_m\lambda_{8,12} + \tfrac{1}{8}d_m{}^2\lambda_{2,22} - \tfrac{1}{8}\mu_m d_m{}^2\lambda_{7,122} = 0. \quad (15)$$

$$-\lambda_2 - \frac{\rho_f d_f}{h}\ddot{u}_{02}{}^f + \frac{3}{8}\frac{\rho_f d_f{}^3}{h}\ddot{\phi}_2{}^f + \frac{\mu_f d_f}{h}u^f_{02,11} - \frac{3}{8}\frac{\mu_f d_f{}^3}{h}\phi^f_{2,11} + \frac{\mu_f d_f}{h}\psi^f_{1,1}$$
$$+ \mu_f\lambda_{7,1} - \tfrac{1}{2}d_f\lambda_{4,2} + \tfrac{1}{2}\mu_f d_f\lambda_{8,12} - \tfrac{1}{8}d_f{}^2\lambda_{2,22} + \tfrac{1}{8}\mu_f d_f{}^2\lambda_{7,122} = 0. \quad (16)$$

$$-\frac{\mu_m d_m}{h}\psi_1{}^m - \frac{\mu_m d_m}{h}u^m_{02,1} + \frac{3}{8}\frac{\mu_m d_m{}^3}{h}\phi^m_{2,1} - \tfrac{1}{2}d_m\lambda_3 + \mu_m\lambda_7 - \frac{1}{12}\frac{\rho_m d_m{}^3}{h}\ddot{\psi}_1{}^m$$
$$+ \frac{1}{12}\frac{E_m d_m{}^3}{h}\psi^m_{1,11} + \frac{1}{4}\frac{\lambda_m d_m{}^3}{h}\phi^m_{2,1} + \tfrac{1}{2}\lambda_m d_m\lambda_{6,1} + \tfrac{1}{4}d_m{}^2\lambda_{1,2} - \tfrac{1}{2}\mu_m d_m\lambda_{8,2}$$
$$- \tfrac{1}{4}\lambda_m d_m{}^2\lambda_{5,12} + \tfrac{1}{8}\mu_m d_m{}^2\lambda_{7,22} = 0. \quad (17)$$

$$-\frac{\mu_f d_f}{h}\psi_1{}^f - \frac{\mu_f d_f}{h}u^f_{02,1} + \frac{3}{8}\frac{\mu_f d_f{}^3}{h}\phi^f_{2,1} - \tfrac{1}{2}d_f\lambda_3 - \mu_f\lambda_7 - \frac{1}{12}\frac{\rho_f d_f{}^3}{h}\ddot{\psi}_1{}^f$$
$$+ \frac{1}{12}\frac{E_f d_f{}^3}{h}\psi^f_{1,11} + \frac{1}{4}\frac{\lambda_f d_f{}^3}{h}\phi^f_{2,1} + \tfrac{1}{2}\lambda_f d_f\lambda_{6,1} - \tfrac{1}{4}d_f{}^2\lambda_{1,2} - \tfrac{1}{2}\mu_f d_f\lambda_{8,2}$$
$$+ \tfrac{1}{4}\lambda_f d_f{}^2\lambda_{5,12} - \tfrac{1}{8}\mu_f d_f{}^2\lambda_{7,22} = 0. \quad (18)$$

$$-\frac{E_m d_m}{h}\psi_2{}^m - \frac{\lambda_m d_m}{h}u^m_{01,1} + \frac{3}{8}\frac{\lambda_m d_m{}^3}{h}\phi^m_{1,1} - \tfrac{1}{2}d_m\lambda_4 + E_m\lambda_5 - \frac{1}{12}\frac{\rho_m d_m{}^3}{h}\ddot{\psi}_2{}^m$$
$$+ \frac{1}{12}\frac{\mu_m d_m{}^3}{h}\psi^m_{2,11} + \frac{1}{4}\frac{\mu_m d_m{}^3}{h}\phi^m_{1,1} + \tfrac{1}{2}\mu_m d_m\lambda_{8,1} + \tfrac{1}{4}d_m{}^2\lambda_{2,2} - \tfrac{1}{2}E_m d_m\lambda_{6,2}$$
$$- \tfrac{1}{4}\mu_m d_m{}^2\lambda_{7,12} + \tfrac{1}{8}E_m d_m{}^2\lambda_{5,22} = 0. \quad (19)$$

$$-\frac{E_f d_f}{h}\psi_2{}^f - \frac{\lambda_f d_f}{h}u^f_{01,1} + \frac{3}{8}\frac{\lambda_f d_f{}^3}{h}\phi^f_{1,1} - \tfrac{1}{2}d_f\lambda_4 - E_f\lambda_5 - \frac{1}{12}\frac{\rho_f d_f{}^3}{h}\ddot{\psi}_2{}^f$$
$$+ \frac{1}{12}\frac{\mu_f d_f{}^3}{h}\psi^f_{2,11} + \frac{1}{4}\frac{\mu_f d_f{}^3}{h}\phi^f_{1,1} + \tfrac{1}{2}\mu_f d_f\lambda_{8,1} - \tfrac{1}{4}d_f{}^2\lambda_{2,2} - \tfrac{1}{2}E_f d_f\lambda_{6,2}$$
$$+ \tfrac{1}{4}\mu_f d_f{}^2\lambda_{7,12} - \tfrac{1}{8}E_f d_f{}^2\lambda_{5,22} = 0. \quad (20)$$

$$-\frac{3}{4}\frac{\mu_m d_m{}^3}{h}\phi_1{}^m - \frac{1}{4}\frac{\mu_m d_m{}^3}{h}\psi^m_{2,1} - \tfrac{1}{8}d_m{}^2\lambda_1 - \tfrac{3}{2}\mu_m d_m\lambda_8 - \frac{49}{320}\frac{\rho_m d_m{}^5}{h}\ddot{\phi}_1{}^m$$
$$+ \frac{3}{8}\frac{\rho_m d_m{}^3}{h}\ddot{u}_{01}{}^m + \frac{49}{320}\frac{E_m d_m{}^5}{h}\phi^m_{1,11} - \frac{3}{8}\frac{E_m d_m{}^3}{h}u^m_{01,11} - \frac{3}{8}\frac{\lambda_m d_m{}^3}{h}\psi^m_{2,1}$$
$$+ \tfrac{1}{8}\lambda_m d_m{}^2\lambda_{5,1} + \tfrac{3}{4}\mu_m d_m{}^2\lambda_{7,2} = 0. \quad (21)$$

$$-\frac{3}{4}\frac{\mu_f d_f{}^3}{h}\phi_1{}^f - \frac{1}{4}\frac{\mu_f d_f{}^3}{h}\psi^f_{2,1} + \tfrac{1}{8}d_f{}^2\lambda_1 - \tfrac{3}{2}\mu_f d_f\lambda_8 - \frac{49}{320}\frac{\rho_f d_f{}^5}{h}\ddot{\phi}_1{}^f$$
$$+ \frac{3}{8}\frac{\rho_f d_f{}^3}{h}\ddot{u}_{01}{}^f + \frac{49}{320}\frac{E_f d_f{}^5}{h}\phi^f_{1,11} - \frac{3}{8}\frac{E_f d_f{}^3}{h}u^f_{01,11} - \frac{3}{8}\frac{\lambda_f d_f{}^3}{h}\psi^f_{2,1}$$
$$- \tfrac{1}{8}\lambda_f d_f{}^2\lambda_{5,1} - \tfrac{3}{4}\mu_f d_f{}^2\lambda_{7,2} = 0. \quad (22)$$

$$-\frac{3}{4}\frac{E_m d_m^3}{h}\phi_2{}^m - \frac{1}{4}\frac{\lambda_m d_m^3}{h}\psi^m_{1,1} - \tfrac{1}{8}d_m\lambda_2 - \tfrac{3}{2}E_m d_m\lambda_6 - \frac{49}{320}\frac{\rho_m d_m^5}{h}\ddot{\phi}_2{}^m$$
$$+\frac{3}{8}\frac{\rho_m d_m^3}{h}\ddot{u}_{02}{}^m + \frac{49}{320}\frac{\mu_m d_m^5}{h}\phi^m_{2,11} - \frac{3}{8}\frac{\mu_m d_m^3}{h}\psi^m_{1,1} - \frac{3}{8}\frac{\mu_m d_m^3}{h}u^m_{02,11}$$
$$+\tfrac{1}{8}\mu_m d_m{}^2\lambda_{7,1} + \tfrac{3}{4}E_m d_m{}^2\lambda_{5,2} = 0. \tag{23}$$

$$-\frac{3}{4}\frac{E_f d_f^3}{h}\phi_2{}^f - \frac{1}{4}\frac{\lambda_f d_f^3}{h}\psi^f_{1,1} + \tfrac{1}{8}d_f{}^2\lambda_2 - \tfrac{3}{2}E_f d_f\lambda_6 - \frac{49}{320}\frac{\rho_f d_f^5}{h}\ddot{\varphi}_2{}^f$$
$$+\frac{3}{8}\frac{\rho_f d_f^3}{h}\ddot{u}_{02}{}^f + \frac{49}{320}\frac{\mu_f d_f^5}{h}\phi^f_{2,11} - \frac{3}{8}\frac{\mu_f d_f^3}{h}\psi^f_{1,1} - \frac{3}{8}\frac{\mu_f d_f^3}{h}u^f_{02,11}$$
$$-\tfrac{1}{8}\mu_f d_f{}^2\lambda_{7,1} - \tfrac{3}{4}E_f d_f{}^2\lambda_{5,2} = 0, \tag{24}$$

which, with the interface compatibility equations (2)–(7), constitutes a system of twenty differential equations in the dependent variables $u_{0i}{}^m$, $u_{0i}{}^f$, $\psi_i{}^m$, $\psi_i{}^f$, $\phi_i{}^m$, $\phi_i{}^f$, $i = 1, 2$, and $\lambda_j, j = 1, 2, \ldots, 8$.

3. WAVE PROPAGATION RESULTS

We now investigate the behavior of time-harmonic waves in an infinite medium for a variety of propagation directions and propagation modes, placing particular emphasis on examining mode shape profiles rather than dispersion spectra alone (reasons for this become apparent in the discussion of the results).

We use as an example the composite previously used by Sun, Achenbach and Herrmann [1] in their original derivation of the effective stiffness theory. Thus we consider a laminated medium with the following properties: for the reinforcing material, $\lambda_f = 50{\cdot}0$ g/cm-μsec^2, $\mu_f = 33{\cdot}33$ g/cm-μsec^2, $\rho_f = 1{\cdot}0$ g/cm^3, and $d_f = 1{\cdot}0$ cm; for the matrix material, $\lambda_m = 0{\cdot}7777$ g/cm-μsec^2, $\mu_m = 0{\cdot}3333$ g/cm-μ sec^2, $\rho_m = 0{\cdot}3333$ g/cm^3, and $d_m = 0{\cdot}25$ cm. In terms of the notation used in [1], these parameters correspond to $\gamma = \mu_f/\mu_m = 100{\cdot}0$, $\theta = \rho_f/\rho_m = 3{\cdot}0$, $\eta = d_f/h = 0{\cdot}8$, $v_f = \lambda_f/2(\lambda_f + \mu_f) = 0{\cdot}3$, $v_m = \lambda_m/2(\lambda_m + \mu_m) = 0{\cdot}35$, $\xi = hd_f = k$, and $\beta = (\omega/k)/\sqrt{(\mu_m\rho_m)} = \omega/k$. In this case, ω and k are respectively, the circular frequency and the wave number (2π/wavelength).

The dependent variables in the equations of motion are assumed to have solutions of the following form:

$$\alpha(x_1, x_2, t) = A \exp i(kn_1x_1 + kn_2x_2 \pm \omega t),$$

which reduces the system of equations to a set of twenty linearly-dependent homogeneous algebraic equations. The dispersion relation and the relative amplitudes of each dependent variable are given by the eigenvalues and eigenvectors of the matrix of the coefficients.

By substituting the resulting values of the dependent variables into equation (1) in combination with the usual linear elastic constitutive equations, the various components of displacement and stress can be evaluated. However, one important step in this process which sheds light on the nature of the theory, requires careful attention. To calculate a particular mode shape one must first choose a point in the medium and designate it as lying on the center line of either the matrix or reinforcing material. If, for example, the matrix material is chosen, the matrix variables are evaluated at this point. It then is necessary to

designate a new point at a distance $(d_m + d_f)/2$ along the x_2 direction as lying on the center line of the adjacent reinforcing layer and evaluate the reinforcing variables at this new point.

The results of this analysis are compared to corresponding results calculated using the theory of elasticity equations presented by Sve[11]. The results from elasticity theory, particularly the mode results, have intrinsic interest and importance in addition to their usefulness for comparisons. Such mode data has been presented for waves propagating parallel to the layers[12], but we believe this is the first published mode data for other propagation directions.

Since we have assumed that the solutions are independent of the x_3 coordinate, the horizontally polarized shear modes in the x_1–x_3 plane are excluded from our results. However, the microstructure theory still admits four modes of propagation having real wave numbers for each propagation direction, i.e. one acoustic and one optical branch for both longitudinal and vertically polarized shear deformation.

Three directions of propagation will be considered. They are: (1) propagation in the direction of the layering ($n_1 = 1$ and $n_2 = 0$); (2) propagation at 45° to the layering ($n_1 = n_2 = 1/\sqrt{2}$); (3) propagation perpendicular to the layering ($n_1 = 0$ and $n_2 = 1$). The dispersion spectra for these cases are shown in Figs. 2–4. For cases (1) and (2) at low wave number, the lowest mode is a shear mode followed by two longitudinal modes and finally a shear mode. For case (3) the lowest mode is shear followed by longitudinal, shear, and longitudinal modes. It should be noted that for case (2), the shear and longitudinal motions are strongly coupled, making the classification of these modes somewhat subjective.

The theory of elasticity solutions are also shown in these figures. In general, the agreement between the dispersion curves of the two theories is quite good. However, as will be discussed later, this does not necessarily indicate that the microstructure theory is adequately modeling the actual response of the material. Finally, it should be emphasized that in some cases the elasticity equations yield additional propagation modes which fall between the modes shown in the figures. Only those elasticity modes which seem to correspond most closely to the microstructure modes have been included in the figures for comparison.

We will begin the discussion of the mode shape comparisons by first considering the

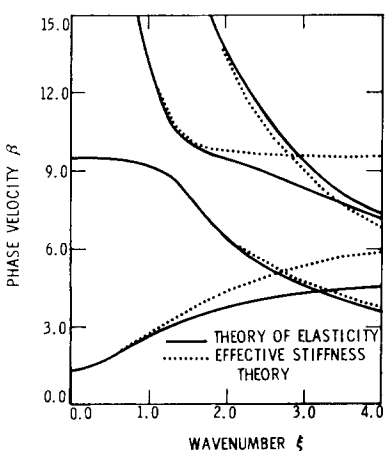

Fig. 2. Dispersion spectrum for propagation in direction of the layering.

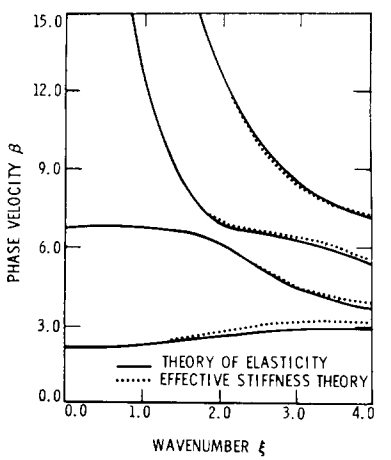

Fig. 3. Dispersion spectrum for propagation at 45° to the layering.

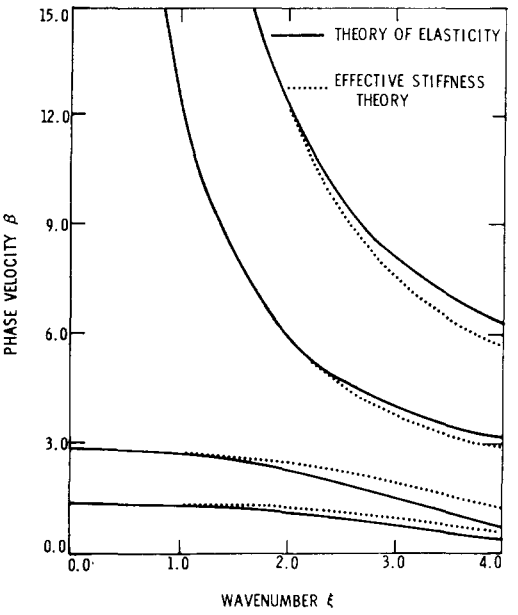

Fig. 4. Dispersion spectrum for propagation perpendicular to the layering.

simpler directions of propagation, cases (1) and (3). In case (3) for propagation perpendicular to the layering, an illustrative example of a longitudinal wave in the second mode which moves from left to right along the x_2 direction is shown in Figs. 5 and 6. The frequency for this case falls in the neighborhood of the first cut-off frequency of the elasticity solution, i.e. that frequency above which waves will only propagate with exponentially decaying amplitudes. This region provides a relatively severe test of the theory.

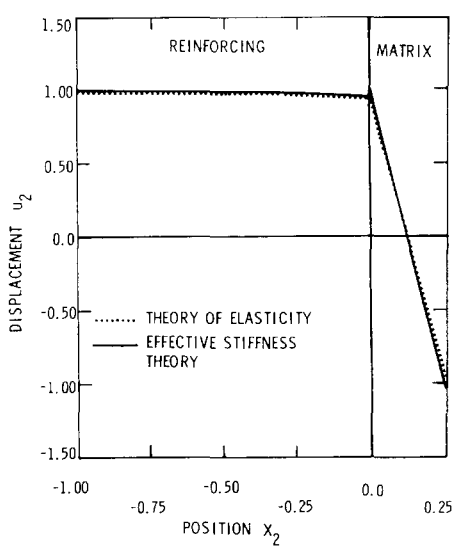

Fig. 5. Lowest longitudinal mode propagating perpendicular to the layering, $\xi = 2$.

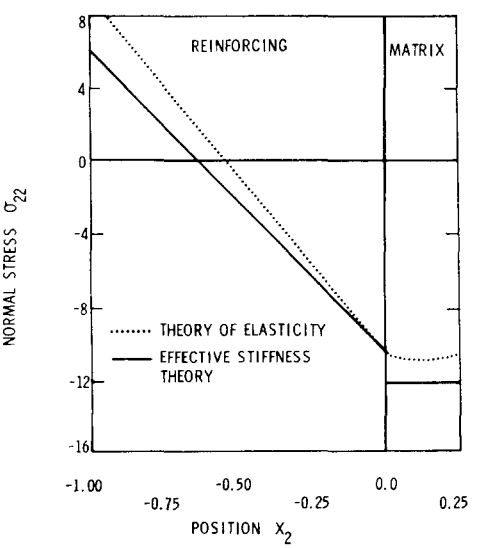

Fig. 6. Lowest longitudinal mode propagating perpendicular to the layering, $\xi = 2$.

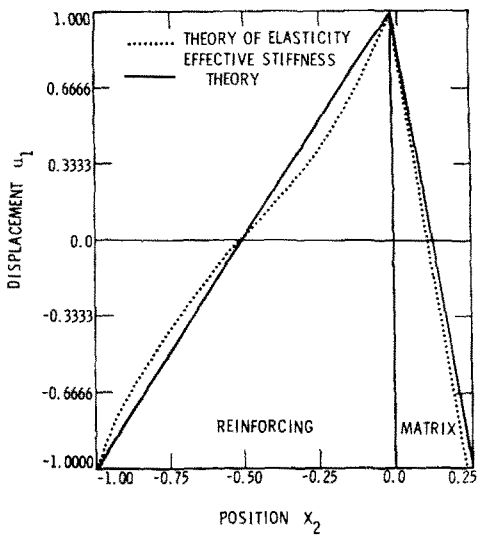

Fig. 7. Lowest shear mode propagating in the direction of the layering, $\xi = 2$.

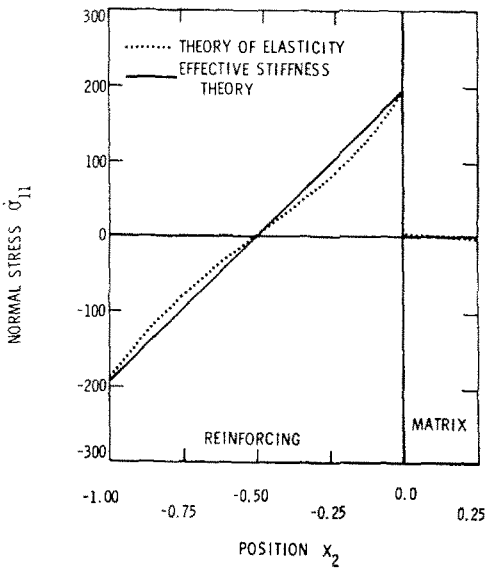

Fig. 8. Lowest shear mode propagating in the direction of the layering, $\xi = 2$.

We can immediately note some of the discrepancies between the microstructure and the elasticity results; however, within the microstructure results alone, we also note a deterioration in the continuity of displacement and stress across the material interface. Still, considering that we are looking at a relatively short wavelength, the agreement may be acceptable for particular applications.

The next case, case (1), is for waves propagating in the direction of the layering. These waves travel out of the page along the x_1 direction in Figs. 7–10. Because the waves are

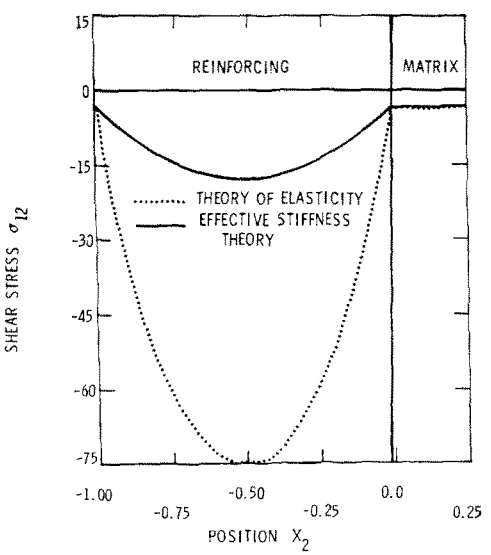

Fig. 9. Lowest shear mode propagating in the direction of the layering, $\xi = 2$.

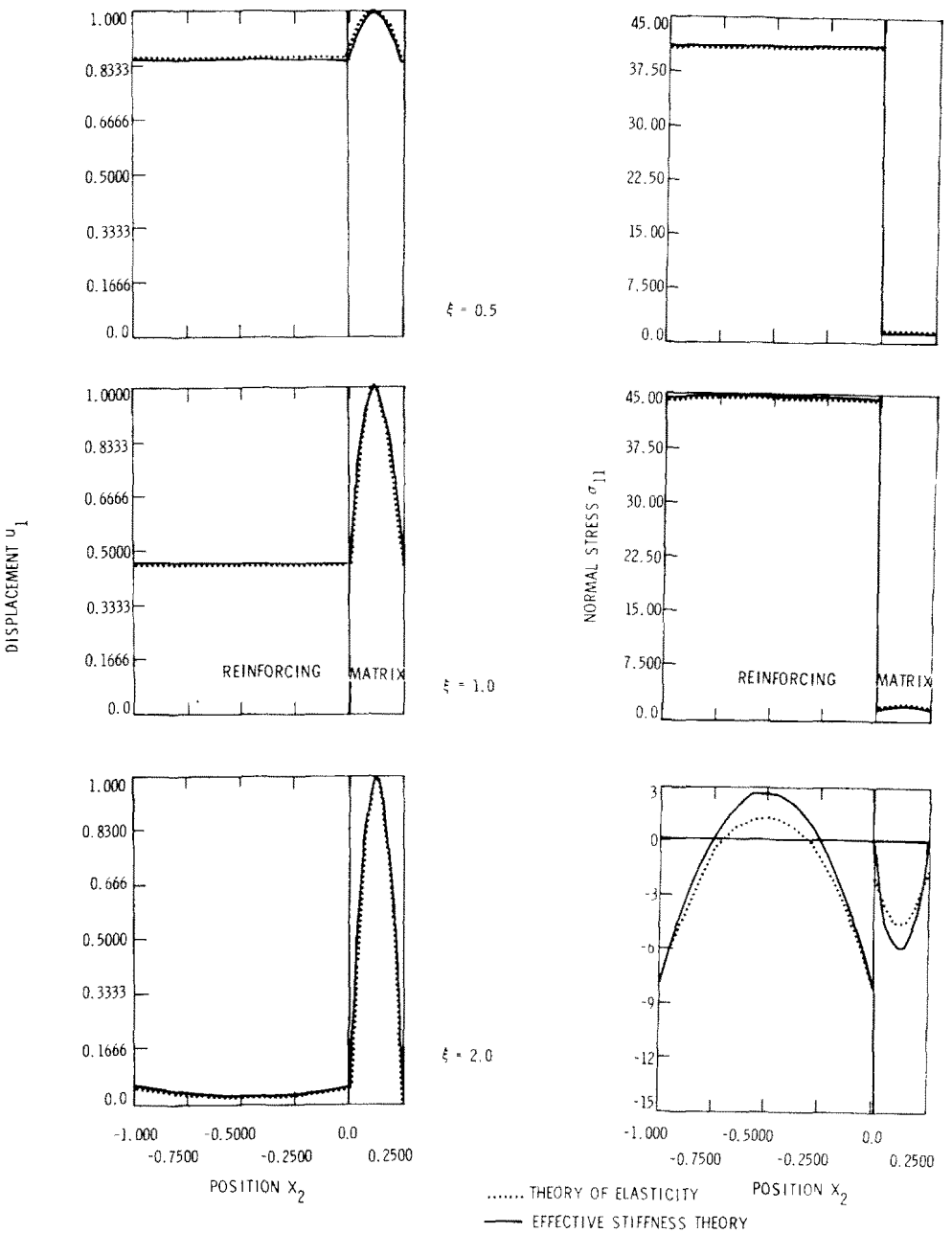

Fig. 10. Lowest longitudinal mode propagating in the direction of the layering.

propagating in the x_1 direction alone, the microstructure interface–continuity conditions will always be satisfied. Thus, unlike the previous case, we do not see a break in the curves of those quantities which should be continuous across the interface.

Figures 7–9 represent the lowest shear mode for $\xi = 2.0$. As seen in Fig. 2, there is considerable error in the phase velocity for this case. Even so, the displacements and normal stresses are in good agreement. The greatest difference occurs in the shear stress comparison.

Figure 10 shows comparisons of displacement and normal stress for several values of wave number in the lowest longitudinal mode. (For $\xi = 4$, which is not shown, the plots are identical to those for $\xi = 2$.) Examination of this figure reveals some interesting characteristics of the effects of increasing wave number, particularly the change in the stress plots from $\xi = 1$ to $\xi = 2$. Comparison between theories is good for this case. (Although it has not been shown, the comparison for shear stress is also good.)

The last case to be discussed, waves propagating at 45° to the layering, is extremely difficult to visualize. For this reason, we have made use of a three dimensional plotting technique which makes possible clear and illuminating qualitative comparisons between the stresses and displacements predicted by the microstructure theory and those obtained from elasticity theory.

We begin by slicing out a section of the layered medium as shown in Fig. 11. The wave will propagate from left to right, perpendicular to the vertical grid lines. Two complete

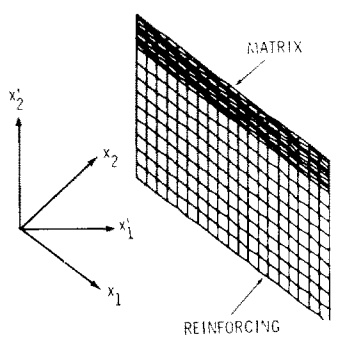

Fig. 11. Plotting surface for waves propagating at 45° to the layering.

plate thicknesses are shown, each divided into nine equal sections by the sloping grid lines. Two overlapping grid lines have been placed at the plate interface in order to represent discontinuities at this junction. We will now rotate this object 90° about the x_1' axis, so that the matrix plate with the narrowly spaced grid lines is placed farthest away from the viewer. The surface now appears as a horizontal line. In its new orientation, the wave still appears to move from left to right and this surface can now be distorted in the vertical direction to illustrate any one of the two components of displacement or three components of stress. Please note, however, that we will still plot values of these functions evaluated in the x_1–x_2 coordinate system.

For wave number $\xi = 2$, samples of components of stress and displacement are shown in Figs. 12–15 from all four modes. For example, at the top of Fig. 12, we show the u_1

displacement for the lowest shear mode. On the left is the theory of elasticity prediction. On the right is the microstructure prediction. (Note the discontinuity in u_1 at the interface.)

The second and third modes, in Figs. 13 and 14, appear to have the best comparison between the elasticity and microstructure solutions. They were previously labeled longitudinal modes. Note that in mode two, the two plates move in-phase while the opposite is true in mode three. Mode one, Fig. 12, has the next best agreement. The principle deviations occur in the σ_{11} comparisons.

It is interesting to look back at Fig. 3 and note the excellent agreement in the dispersion spectra of mode four. On the basis of dispersion data alone, one would have concluded that mode four was adequately modeled. However, the largest differences in the mode shapes occur in mode four.

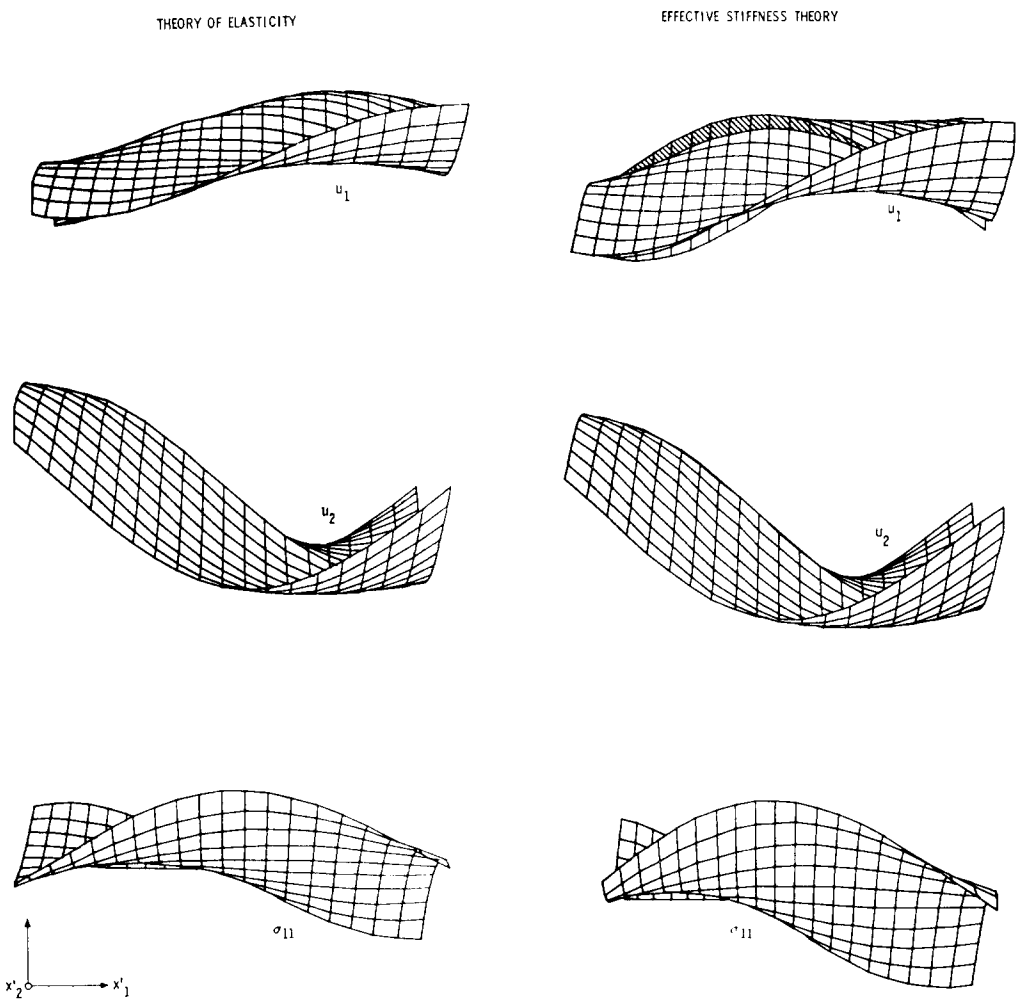

Fig. 12. Comparison of mode shape profiles for first mode propagating at 45° to layering.

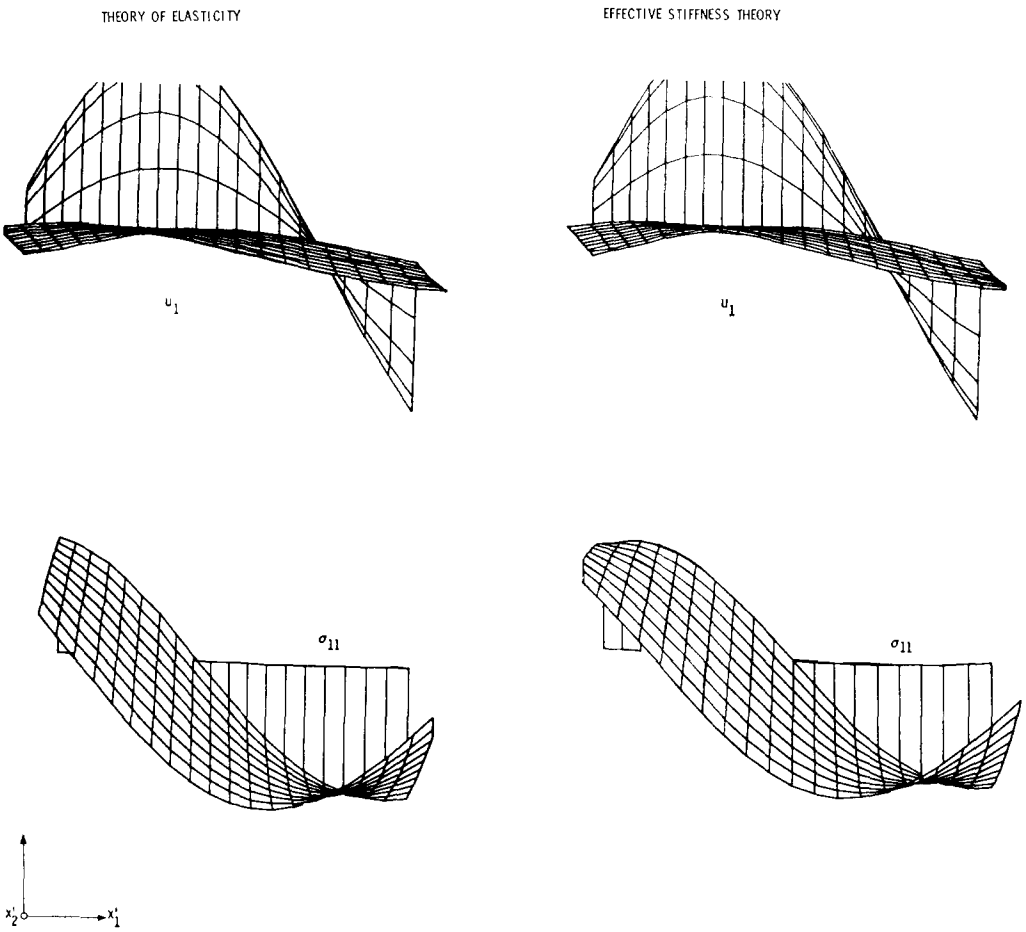

Fig. 13. Comparison of mode shape profiles for second mode propagating at 45° to layering.

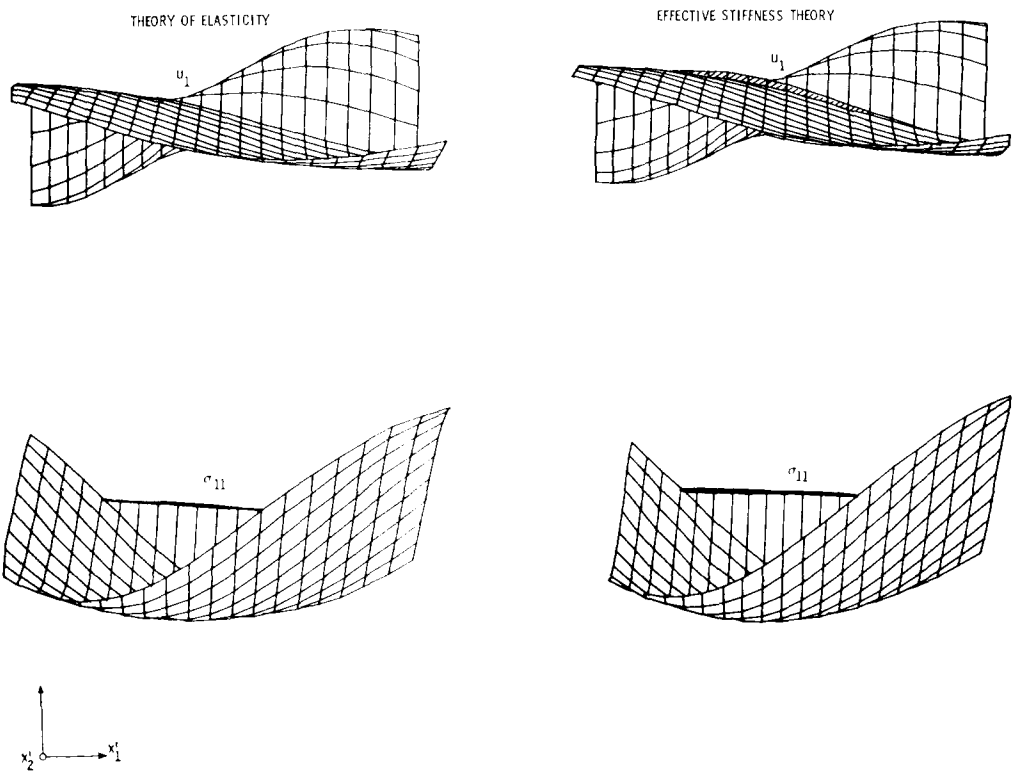

Fig. 14. Comparison of mode shape profiles for third mode propagating at 45° to layering.

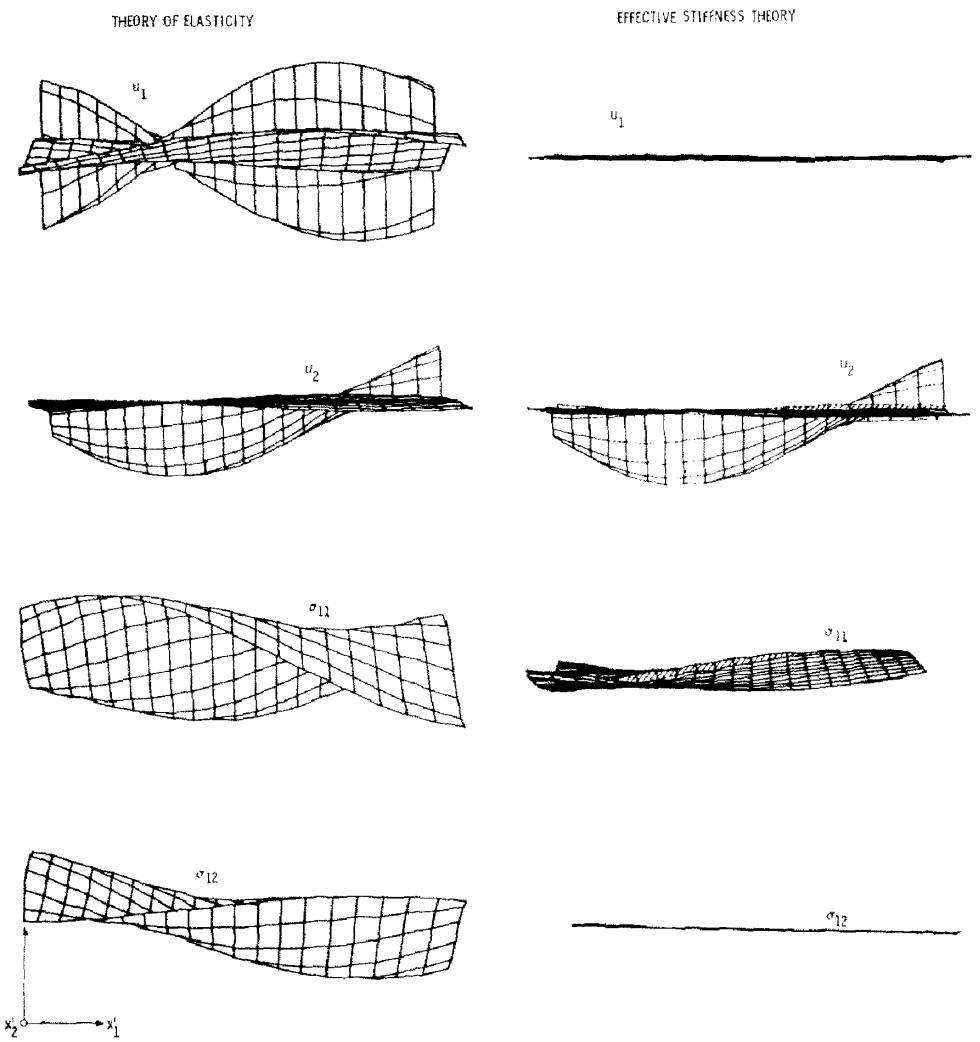

Fig. 15. Comparison of mode shape profiles for fourth mode propagating at 45° to layering.

4. CONCLUSIONS

On the basis of our results, we have determined that a second order effective stiffness theory is capable of predicting with reasonable accuracy the stress and displacement distributions associated with several of the lowest theory of elasticity modes. As would naturally be anticipated, the accuracy deteriorated with increasing frequency, and marked discrepancies occur between mode prediction at the higher modes which would have to be considered in applying the theory to particular problems.

Finally, we have given strong evidence that dispersion comparisons alone cannot constitute a valid criteria for the assessment of a microstructure theory.

Acknowledgements—We wish to express our appreciation to E. G. Young for her invaluable help in plotting the figures contained in this report.

REFERENCES

1. C.-T. Sun, J. D. Achenbach and G. Herrmann, Continuum theory for a laminated medium. *J. appl. Mech.* **35**, 467–475 (1968).
2. C.-T. Sun, J. D. Achenbach and G. Herrmann, On the vibration of a laminated body. *J. appl. Mech.* **35**, 689–696 (1968).
3. J. D. Achenbach and G. Herrmann, Wave motion in solids with lamellar structuring. *Dynamics of Structured Solids*, p. 23. American Society of Mechanical Engineers (1968).
4. J. D. Achenbach and G. Herrmann, Effective stiffness theory for a laminated composite. *Proceedings of the 10th Midwestern Mechanics Conference*. Johnson Publishing Company, pp. 91–106 (1968).
5. G. Herrmann and J. D. Achenbach, Applications of theories of generalized cosserat continua to the dynamics of composite materials. *Mechanics of Generalized Continua*. Springer, pp. 69–79 (1968).
6. G. Herrmann and J. D. Achenbach, Wave propagation in laminated and fiber-reinforced composites. *Mechanics of Composite Materials*. Pergamon Press, pp. 337–360 (1970).
7. J. D. Achenbach and C.-T. Sun, The directionally reinforced composite as a homogeneous continuum with microstructure. *Dynamics of Composite Materials*, pp. 48–69. American Society of Mechanical Engineers (1972).
8. G. A. Hegemier, On a theory of interacting continua for wave propagation in composites. *Dynamics of Composite Materials*, pp. 70–121. American Society of Mechanical Engineers (1972).
9. C. Truesdell and W. Noll, The non-linear field theories of mechanics, *Handbuch der Physik*, Vol. III/3. Springer (1965).
10. D. S. Drumheller and A. Bedford, On a continuum theory for a laminated medium. *J. appl. Mech.* **40**, 527–532 (1973).
11. C. Sve, Time harmonic waves travelling obliquely in a periodically laminated medium. *J. appl. Mech.* **38**, 477–482 (1971).
12. O. Hoffman, Study of advanced filament-reinforced materials final report, Lockheed Report No. LMSC-D244187 (1972).